Modeling and Analysis of a Ceramic matrix composites with strain induced damage using F. E. Method

Dr. Ratnakar Pandu[1], Professor of Mechanical Engineering, Email: dr.ratnakarpandu@gmail.com

St. Martin's Engineering College, Hyderabad, A.P, INDIA

ABSTRACT:

A computationally efficient FE model has been developed to predict the mechanical behavior of ceramic matrix composites with strain-induced damage. The effects of different damage modes and their interactions on mechanical behavior have been considered. The non-linear longitudinal material properties are discretised to a multi-linear elastic curve. The constitutive equations for orthotropic materials are used to update the stresses for each increment of the analysis. The model is implemented by a Finite Element package, ANSYS with a user defined subroutine, UMAT. In all analyses, the expected mechanical behavior has been obtained. Strain induced damage modes and their interactions are modeled using the finite element method for Ceramic Matrix Composites (CMC) tows and 0º/90º laminates. For both situations, bi-axial straining is addressed, together with the degradation of Young's moduli and Poisson's ratios. In all cases, the expected stress-strain behavior is calculated.

Keywords: Finite Element Method; Damage Mechanisms; Ceramic Matrix Composites; Tows; Orthotropic Material.

1. INTRODUCTION

The superior material properties of Ceramic Matrix Composites (CMCs), e.g. low density and good mechanical and thermal properties at high temperatures make them favorable materials for use in: rocket nozzles; thermal protection systems; and gas turbine engines [1]. To perform optimal design of these engineering components, a highly efficient yet computational accurate model is a necessary requirement, due to the complex spatial topology and interactive damage mechanisms of woven CMCs. A finite element (FE) model of unit cell geometry is a commonly used approach to study the behavior of CMCs. Sheikh *et al.* [2] employed a micro-structural FE model to predict steady-state and transient heat conduction for the plain weave DLR-XT composite. Deepak and Whitcomb [3] evaluated load flow in plain weave composites by using a detailed 3D FE model and a non-standard post-processing technique. Although the full FE analysis is capable of predicting accurate micromechanical responses, it is computationally expensive because a precise description of the geometry is required.

In order to tackle practical problems in the design and analysis of composites, some computationally efficient FE models have been developed. Tanov and Tabiei [4] predicted the equivalent material properties of plain weave fabric composites by homogenizing an entire unit cell model. Cox *et al.* [5] introduced a Binary Model, which is composed of two virtual components: a 1D truss element and a 3D solid element. Whilst the Binary Model has great simplicity, it does require accurate determination of the mechanical and thermal properties of the two virtual components. However, an alternative simpler and more accurate approach has been adopted here. For all of these approaches, the material properties are assumed to be linear elastic. The present paper addresses the development of a conceptually simple and computationally economic FE model, which emphasizes the effects of strain-induced damage modes and their interactions on the mechanical behavior. Non-linear material properties are modeled by multi-linear elastic Discretization. A unidirectional tow is homogenized to a single orthotropic block. Multi-axial stress-strain response and degradation of material properties are modeled for unidirectional tows and 0º/90º laminates.

2. DAMAGE MODES AND MECHANICAL BEHAVIOR OF A UNIDIRECTIONAL TOW

The damage modes and typical mechanical behavior of a unidirectional tow subjected to different loading conditions are described in this section. The interactions of different damage modes and their effects on the stress-strain response are introduced.

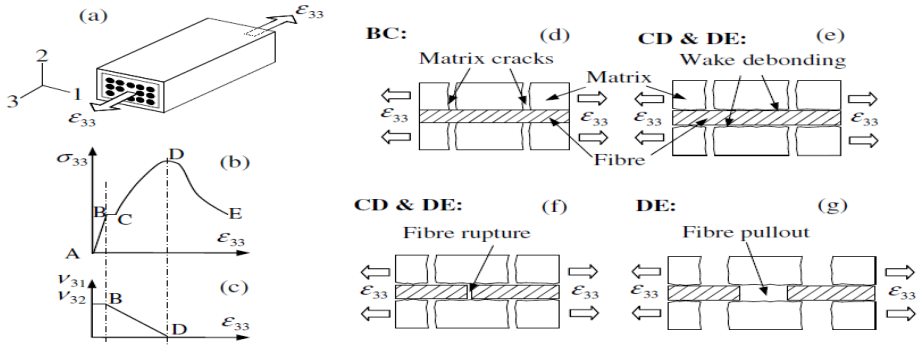

Fig.1. Schematic drawings of (a) A unidirectional tow under longitudinal extension; (b) and (c) Longitudinal stress-strain and Poisson's ratio-strain curves; and (d)–(g) Corresponding damage modes.

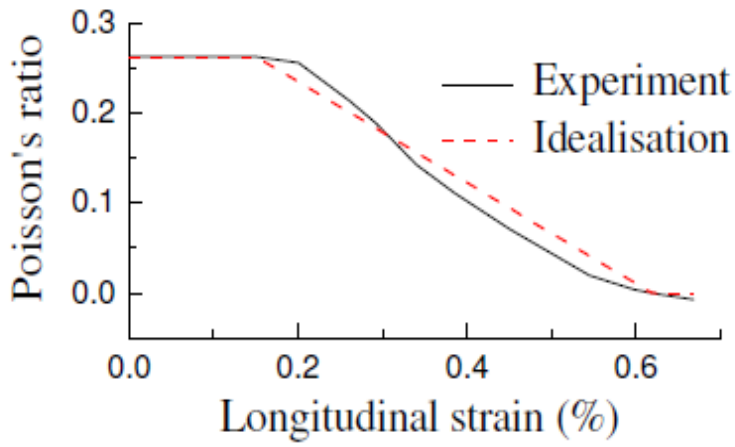

Fig. 2. Measured [8] and assumed variation of Poisson's ratios, ν31 and ν 32 with longitudinal strain.

2.1 Longitudinal extension

When a unidirectional fibre-reinforced ceramic matrix composite tow (single bundle of fibres and associated matrices) is under uniform extension along the fibre direction (Fig.1a), the typical longitudinal stress-strain response [5] (Fig.1b) and Poisson's ratio-longitudinal strain curve (Fig.1c), can be observed. The four characteristic stages in the stress-strain curve are now described [7]:

AB: Initially, the composite behaves as a virgin, undamaged, linear elastic material;

BC: Periodic matrix cracking occurs (Fig.1d);

CD: Fibrematrix interface de-bonding takes place at the matrix crack tip and its wake (wake de-bonding in Fig.1e); and weaker fibres fail (Fig.1f);

DE: The majority of fibres fail and are pulled out against the frictional stress along the wake de-bonding interface (Fig.1g). Fig.2 shows how the Poisson's ratio-longitudinal strain curve in Figure 1c can be idealized from the experimental data [8] for a unidirectional Nicalon/CAS composite. It can be seen that initially, Poisson's ratio is constant, then decreases linearly due to matrix cracking and wake debonding, and finally approaches zero at peak stress D, as shown in Fig.1b.

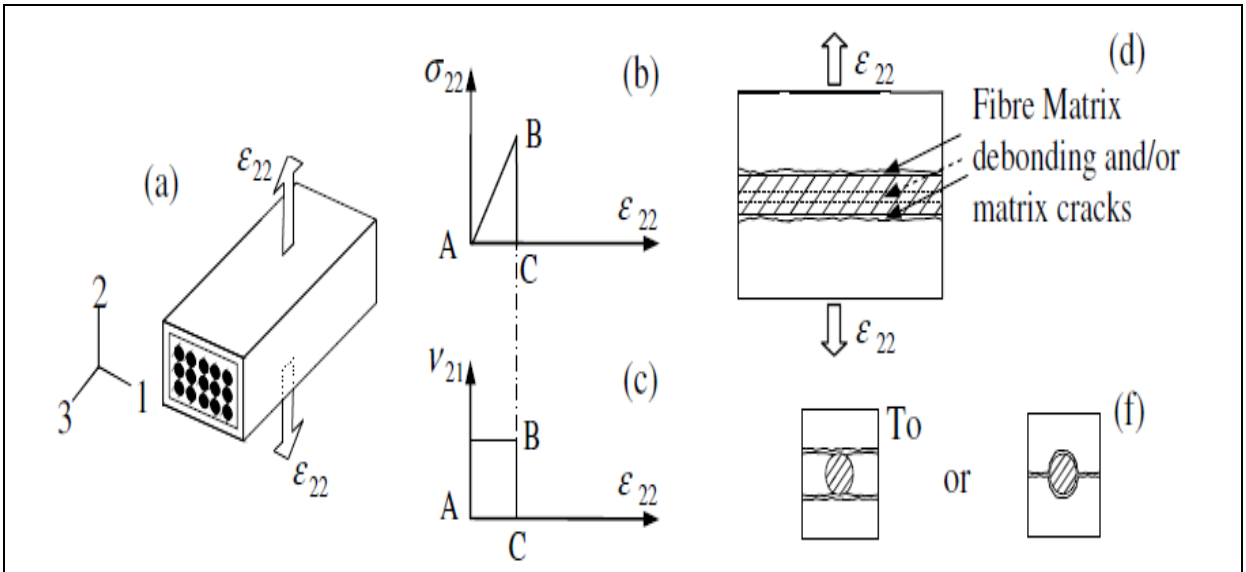

Fig. 3. Schematic drawings of (a) A unidirectional tow under transverse straining; (b) and (c) Transverse stress-strain and Poisson's ratio curves; and (d)–(f) Corresponding damage modes.

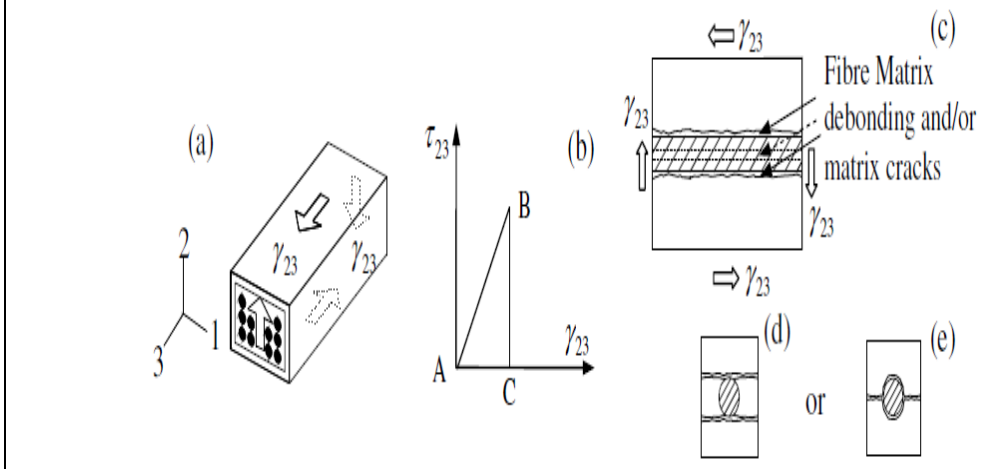

Fig. 4. Schematic drawings of (a) A unidirectional tow under shear straining; (b) and (c) Shear stress-strain curve; and (c)–(e) Corresponding damage modes.

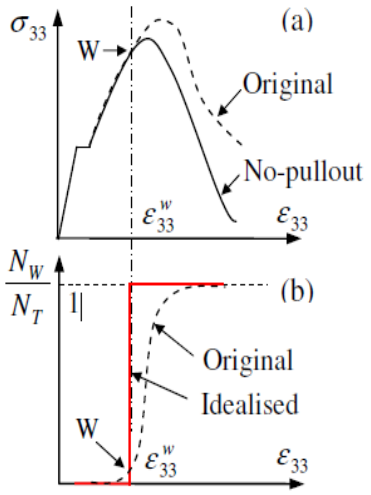

Fig. 5. Schematic drawing of (a) No-pullout stress-strain curve; (b) Variation of the normalized number of wake debonded blocks with longitudinal strain.

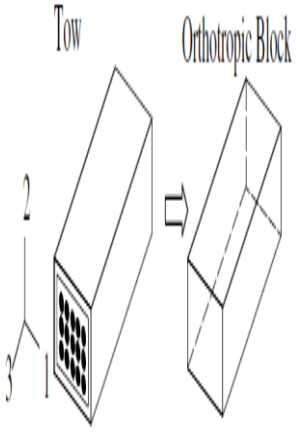

Fig. 6. Homogenization of a unidirectional tow to a single orthotropic block

2.2 Transverse extension

When a unidirectional tow is subjected to transverse extension (Fig.3a), the material response is assumed to be piecewise linear elastic (Fig.3b and 3c). When the global transverse strain reaches a critical value, fibre-matrix debonding and/or matrix cracking (Fig.3d–3f) is assumed to take place which leads to catastrophic failure.

2.3 Shear loading

As can be seen from Fig.4, in the case of shear straining, the shear stress-strain response and damage modes are assumed to have the same form as those for transverse straining.

2.4 Damage interactions and no-pullout curve

When a unidirectional tow is under multi-axial loading, e.g. both longitudinal and transverse straining (ε_{33} and ε_{22}); or both longitudinal and shear straining (ε_{33} and γ_{23}), the interaction between certain damage modes is strong and needs to be considered. The positive transverse stress (σ_{11}) or shear stress (τ_{23}) advances wake debonding, and hence decouples the interaction between fibres and matrix. As a result, the contribution due to fibre pullout has to be deactivated. Fig.5a shows that the

original stress-strain curve degrades to the no-pullout curve due to this damage interaction [5]. The damage interaction results in the change of Poisson's ratios. The broken curve in Fig.5b represents the variation of the normalized number of wake debonded blocks (fibre-matrix between adjacent matrix cracks) in a tow with longitudinal strain [7]. In the present model, it is assumed that all the blocks wake debond at the point, W; namely; the dash curve in Fig.5b is idealized to the solid curve. The strain level at which the deactivation point W occurs has been determined by examination of the original and no-pullout curves (Fig.5a). Consequently, Poisson's ratios ν31 and ν32 drop to zero at the wake debonding strain, □ , when the switch to the no-pullout curve is activated.

3. Formulation Of The Finite Element Model

A unidirectional tow is chosen to be the basic constituent in the FE model, and therefore an entire tow, which consists of thousands of fibres embedded in matrix, can be represented by a single 8-node solid finite element (Fig.6). The material properties are assumed to be multi-linear elastic and the stress-strain and Poisson's ratios-strain curves shown in Fig.1, 3 and 4 are used to develop the constitutive equations. The FE software ANSYS [9] with a user-defined subroutine UMAT is used to carried out the simulation. This method has the benefit of being able to model a tow by a single orthotropic finite element. The approach has the advantage of simplicity relative to the binary system of modeling [5], since it has only one component; and, unlike the binary method, does not suffer from the difficulties associated with the identification of medium properties.

3.1 Homogenization of a unidirectional tow

A heterogeneous unidirectional tow is homogenized to a single block (Fig.6), which has the same overall dimensions and equivalent orthotropic material properties. There are nine independent material properties: Young's moduli: E3, E2, and E1; Poisson's ratios: ν31, ν32, and ν12; Shear moduli: G12, G23, and G13.

3.2 Discretization of the stress-strain curve and constitutive equations

In order to perform a finite element analysis, the non-linear longitudinal stress-strain relationship is discretised to a multi-linear curve. The loading is imposed in terms of the displacement boundary conditions, i.e. displacement controlled rather than load controlled conditions are modeled. The applied displacement is divided into many small increments. For each increment, the constitutive equations for an orthotropic material are:

$$\begin{Bmatrix}\sigma_{11}\\ \sigma_{22}\\ \sigma_{33}\\ \tau_{23}\\ \tau_{13}\\ \tau_{12}\end{Bmatrix} = \begin{bmatrix} \frac{1-\nu_{23}\nu_{32}}{E_2E_3\Delta} & \frac{\nu_{21}+\nu_{23}\nu_{31}}{E_2E_3\Delta} & \frac{\nu_{31}+\nu_{21}\nu_{32}}{E_2E_3\Delta} & 0 & 0 & 0 \\ \frac{\nu_{21}+\nu_{23}\nu_{31}}{E_2E_3\Delta} & \frac{1-\nu_{13}\nu_{31}}{E_1E_3\Delta} & \frac{\nu_{32}+\nu_{12}\nu_{31}}{E_1E_3\Delta} & 0 & 0 & 0 \\ \frac{\nu_{31}+\nu_{21}\nu_{32}}{E_2E_3\Delta} & \frac{\nu_{32}+\nu_{12}\nu_{31}}{E_1E_3\Delta} & \frac{1-\nu_{12}\nu_{21}}{E_1E_2\Delta} & 0 & 0 & 0 \\ 0 & 0 & 0 & G_{23} & 0 & 0 \\ 0 & 0 & 0 & 0 & G_{13} & 0 \\ 0 & 0 & 0 & 0 & 0 & G_{12} \end{bmatrix} \begin{Bmatrix}\varepsilon_{11}\\ \varepsilon_{22}\\ \varepsilon_{33}\\ \gamma_{23}\\ \gamma_{13}\\ \gamma_{12}\end{Bmatrix} \quad (1)$$

$$\text{where } \Delta = \frac{(1-\nu_{12}\nu_{21}-\nu_{23}\nu_{32}-\nu_{13}\nu_{31}-2\nu_{21}\nu_{32}\nu_{13})}{E_1E_2E_3} \text{ and } \nu_{ij} = \frac{E_i}{E_j}\nu_{ji} \ (i,j = 1\text{–}3 \text{ and } i \neq j).$$

3.3 Assumptions of mechanical couplings due to damage interactions

To model the interactions of the different damage modes, the following assumptions are made.

The switch from the original stress-strain curve to the no-pullout curve is triggered by a small finite positive transverse stress, or by a small non-zero shear stress in the 1-3 or 2-3 plane.

Consequently, the Poisson's ratios, v31 and v32 drop to zero at the wake debonding strain, w □ (Fig.5).

3.4 UMAT implementation in ANSYS

The present model is implemented by using the FE software, ANSYS/standard and a user defined subroutine, UMAT. The multi-linear material properties, the constitutive equations, and the mechanical couplings are defined in the UMAT. For every increment, the UMAT reads the strains at each material point and then assigns the corresponding Young's moduli, Poisson's ratios and shear moduli. The constitutive equations are then used to update the stress fields. Solution-dependent Tate variables, STATEV, record different damage modes and control their interactions. Automatic incrementation algorithms and increment redefinition variable, PNEWDT, are continuously updated to ensure that the discretised points are located exactly at the end of the relevant increments.

4. Multi-Axial Tow AND 0º/90º Laminate Behaviour

The current model is used to analyze a unidirectional tow and a 0º/90º laminate under different loading cases. Applications to composite woven unit cells and real engineering components will be pursued as future developments.

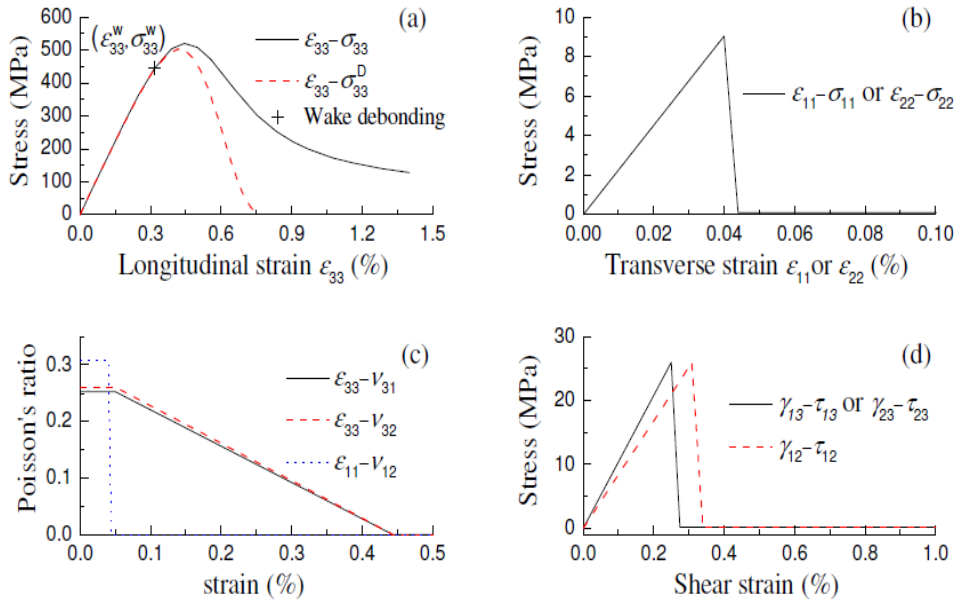

Fig. 7. Material properties of a unidirectional tow.

4.1 Material properties

The material properties of a unidirectional tow of C/C-SiC (Carbon/Carbon-Silcon Carbide) DLR-XT composite are shown in Fig.7. Fig.7a, which is associated with Fig.5a, has been obtained by using the model for a unidirectional tow[7]. The solid curve is the original longitudinal stress-strain relationship, the broken line defines the no-pullout curve, and the cross symbol is the wake debonding point. The initial values of other properties, transverse moduli (Fig.7b), Poisson's ratios (Fig.7c), and shear moduli (Fig.7d) have been calibrated by a fully meshed micro-mechanical FE model. The limit of proportionality of the experimental stress-strain curve for the DLRXT material under uniaxial straining is used to define a transverse failure strain of 0.04% [10]. A value of 26MPa is used to determine the critical shear failure strain [11].

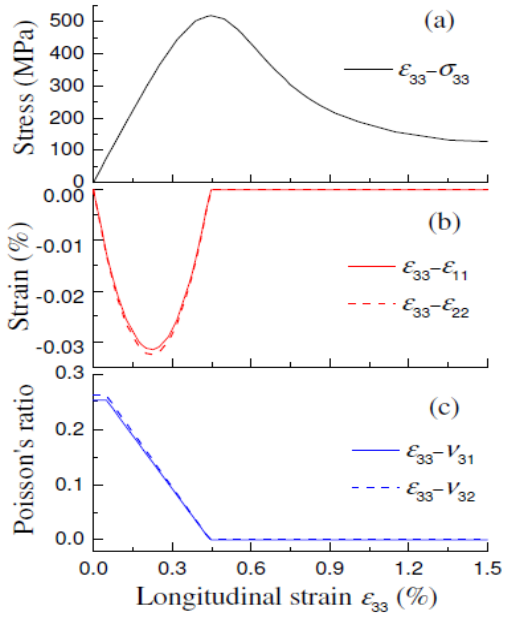

Fig. 8. Finite element results for a unidirectional tow under longitudinal straining (ε33)

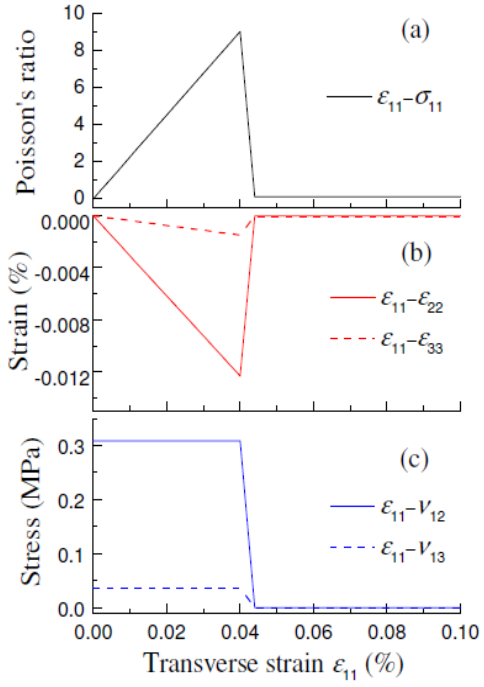

Fig. 9. Finite element results for a unidirectional tow under transverse straining (ε33).

4.2 Unidirectional tow: longitudinal, transverse and shear straining

Fig.8 shows the FE results for a unidirectional tow under longitudinal straining. The stress-strain relationship, longitudinal-transverse strain curves, and variation of Poisson's ratios are plotted in Fig.8a, 8b, and 8c, respectively. As expected, the results are identical to the defined material properties. The results for a unidirectional tow subjected to transverse and shear straining are presented in Fig.9 and 10, respectively. Once again, the method has been validated since input and output values concur.

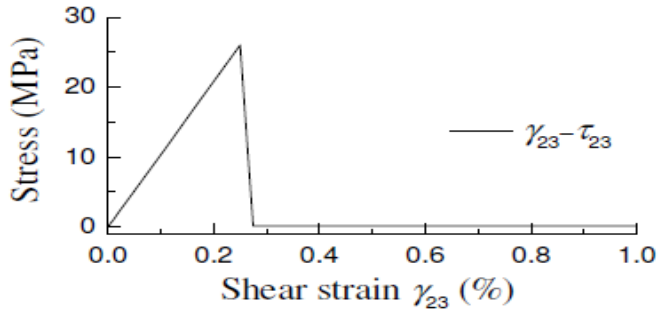

Fig.10. Finite element results for a unidirectional tow under

shear straining.

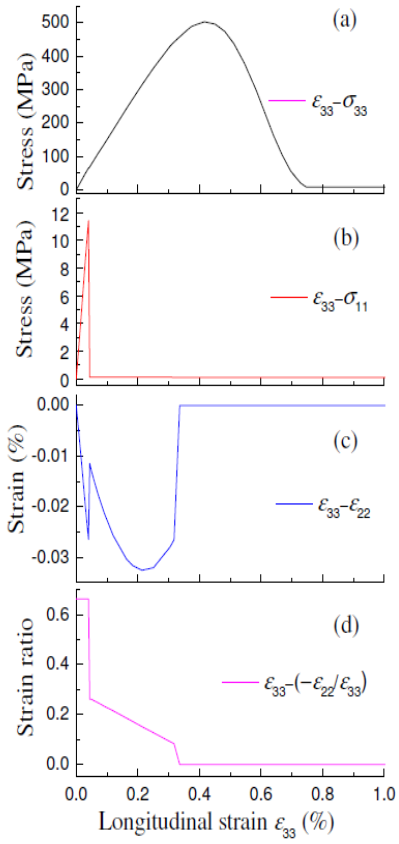

Fig. 11. Finite element results for a unidirectional tow under equibiaxial straining (ε33=ε11).

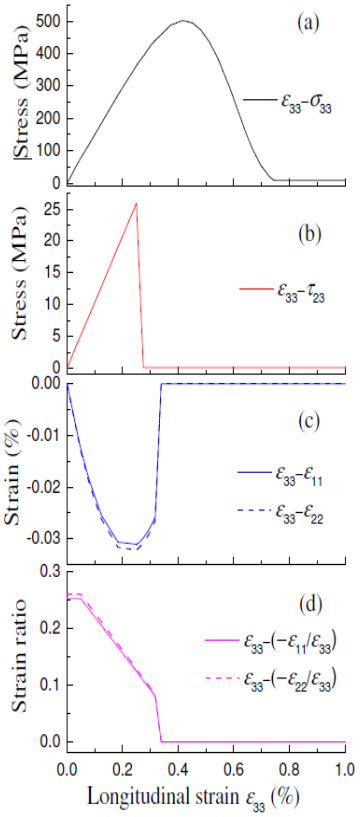

Fig. 12. Finite element results for a unidirectional tow under longitudinal straining (ε33) and shear straining (ε23) with ε33=γ23.

4.3 Unidirectional tow: equibiaxial straining

Fig.11 shows the FE results for a tow under equibiaxial tensile straining, ε33=ε11. From Fig.11a, it can be seen that the no-pullout stress-strain curve is triggered due to the positive stress σ11. Fig.11b shows that the transverse stress, σ11 drops to zero at the defined failure strain (ε11=0.04%). The effect of this transverse failure on the deformation in the other transverse direction is shown as a kink in Fig.11c. The effect can also be seen from the first sharp drop in Fig.11d, which plots the ratio of strains in Fig.11c. The second sharp drop in Fig.11d is due to the second assumption of mechanical coupling, namely that the Poisson's ratio drops to zero at the wake debonding strain.

4.4 Unidirectional tow: combined longitudinal and shear straining

In comparison with the predictions for equibiaxial straining, similar results are obtained for longitudinal and shear straining (Fig.12). In this case, the switch from original to no-pullout curve is triggered by the shear stress. Transverse strains become zero at the wake debonding strain.

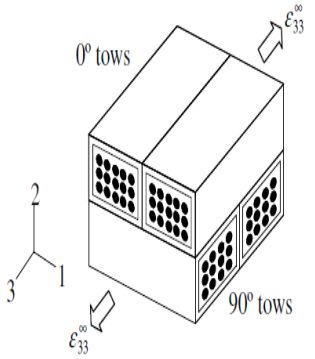

Fig.13. Schematic drawing of a 0°/90° tow laminate under uniaxial straining.

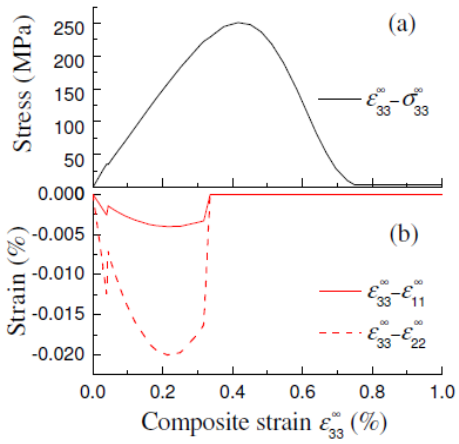

Fig.14. Overall behavior of a 0°/90° laminates under uniaxial straining.

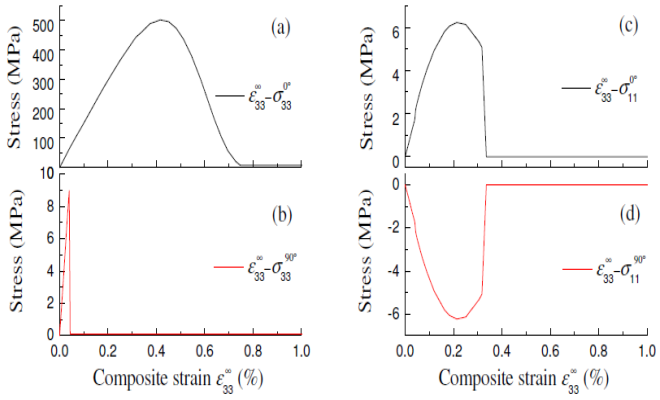

Fig.15. Local behavior of a 0°/90° laminates under uniaxial straining.

4.5. 0º/90º laminates under uniaxial straining

The model is also used to analyze a 0º/90º laminate under in-plane uniaxial straining (Fig. 13). The overall stress-strain response and variations of transverse strains are shown in Fig.14a and 14b, respectively. The kinks at =0.04% in both figures are due to the matrix cracking in the 90º tows. The transverse strains drop to zero at the wake debonding strain, . Fig.15 shows the longitudinal stress-strain and transverse stress-strain response in the different layers. As can be seen from Fig.15a, the no-pullout curve is triggered in the 0º layer. This is because the 0º layer carries a transverse tensile stress (Fig.15c) before the wake debonding strain is reached. This tensile stress is created by the constraint of the 90º layer, since its stiffness in the 1 direction is much higher than that of the 0º layer. In order to satisfy equilibrium, the transverse stress in the 90º layer (Fig.15d) is a mirror of that given in Fig.15c. According to this analysis, even though a 0º/90º laminate is only under in-plane uniaxial tension, the no-pullout curve can still be activated. This is different to the stress-strain response of longitudinal straining of a unidirectional tow.

5. Discussion and conclusions

A computationally efficient FE model has been developed to predict the mechanical behavior of ceramic matrix composites with strain-induced damage. The effects of different damage modes and their interactions on mechanical behavior have been considered. The basic constituent of the FE model is an orthotropic 8-node brick, which forms a homogenized medium of a heterogeneous unidirectional tow. The non-linear longitudinal material properties are discretised to a multi-linear elastic curve. The constitutive equations for orthotropic materials are used to update the stresses for each increment of the analysis. The model is implemented by a commercial FE package, ANSYS with a user defined subroutine, UMAT. Multi-axial stress-strain response and degradation of material properties have been modeled for a unidirectional tow, and for a 0º/90º laminate. In all analyses, the expected mechanical behavior has been obtained. For the 0º/90º laminate under uniaxial straining, the no-pullout stress-strain response in the 0º layer is triggered due to the constraint of the 90º layer. The high efficiency and the simplicity of the model make it possible to analyze large scale woven composites. Application of the model to unit cells and to real engineering components will be pursued as future developments.

6. References

1. Marshall, D. B. and Cox, B. N. 2008 Integral textile ceramic structures. Annu. Rev. Mater. Res., 38, 425–443.
2. Sheikh, M. A., Taylor, S. C., Hayhurst, D. R. and Taylor, R. 2001 Micro structural finite element modeling of a ceramic matrix composite to predict experimental measurements of its macro thermal properties. Model. Simul. Mater. Sci. Eng. 9, 7–23.
3. Deepak, G. and Whitcomb, J. D. 2008 Load flow in plain woven composites. Journal of Composite Materials. 42, 2761–2777.
4. Tanov, R. and Tabiei, A. 2001 Computationally efficient micromechanical models for woven fabric composite elastic moduli. Journal of Applied Mechanics. 68, 53–560.
5. Cox, B. N., Carter, W. C., and Fleck, N. A. 1994 A binary model of textile composites–I. Formulation. Acta Metall. Mater. 42, 3463–3479.
6. Hayhurst, D. R., Leckie, F. A. and Evans, A. 1991 Component design-based model for deformation and rupture of tough fibre-reinforced ceramic matrix composites. Proc. R. Soc. Lond. A. 434, 369–381.
7. Tang, C., Blacklock, M, and Hayhurst, D. R. 2008 Thermo-mechanical behavior of Ceramic Matrix Composites: Part I- Stress-strain response and thermal conductivity degradation of fibre tows. Research report No. DMM.08.04, School of Mechanical, Aerospace and Civil Engineering, the University of Manchester, U.K.
8. Karandikar, P. and Chou, T. 1993 Characterization and modeling of micro cracking and elastic moduli changes in Nicalon/CAS composites. Composites Science and Technology. 46, 253–263.
9. SIMULIA. 2006 ABAQUS user's manual. Version 6.6.
10. Sheikh, M. A., Hayhurst, D.R., Taylor, S. C. and Taylor, R. 2007 Experimental Investigation of the effect of mechanical loading on Thermal Transport in Ceramic Matrix Composites Research report No. DMM. 08.06, School of Mechanical, Aerospace and Civil Engineering, the University of Manchester, U.K.
11. Tang, C., Blacklock, M, and Hayhurst, D. R. 2008 Thermo-mechanical behaviour of Ceramic Matrix Composites: Part II- Stress-strain response and thermal conductivity degradation of fibre tows, 0-90 unidirectional and woven composites. Research report No. DMM. 08.05, School of Mechanical, Aerospace and Civil Engineering, the University of Manchester, U.K.

